https://doi.org/10.5194/nhess-2020-311
Preprint. Discussion started: 3 November 2020

Natural Hazards and Earth System Sciences
Discussions

Extreme marine events revealed by lagoonal sedimentary records in Ghar el Melh during the last 2500 years in the northeast of Tunisia.

Balkis Samah Kohila [1, 2], Laurent Dezileau[2], Soumaya Boussetta [1], Tarek Melki [1], Nejib Kallel. [1]

[1]Laboratoire Géoressouces, Matériaux, Environnements et changements globaux, LR13ES23 (GEOGLOB), Faculté des Sciences de Sfax, BP1171, Sfax 3000, Université de Sfax, Tunisie.
[2]Laboratoire de Morphodynamique Continentale et Côtière (M2C), Université de Caen, UMR 6143, 14000 Caen, France.

Correspondence to: Balkis Samah Kohila (balkis.samah@yahoo.fr)

Abstract. The Tunisian coast has been affected in the past by many events of extreme marine submersion (storms and tsunamis). A high-resolution study along two sediment cores "GEM3" and "GEM4" taken from the lagoon of the Ghar el Melh was performed to identify the different paleo-extreme events and to reconstruct the paleo-environmental changes of the North-eastern part of Tunisia during the Late Holocene. A very high-resolution of analysis (sedimentological, granulometric, and geochemical) was applied on these cores. These cores were also dated with isotopic techniques (^{137}Cs, ^{210}Pbex, ^{14}C) and the outcomes reveal fives phases of paleoenvironmental changes of this lagoonal complex. The first phase dated from -275 to 200 Cal AD characterized by a high percentage of Silt and Clay (fine particles) indicating a protected lagoon. The second phase synchronous with the Dark Age Climatic Period dated from 200 to 1100 Cal AD, is marked by an increase in the coarse sediment and could be explained by a weakening of the sandy barrier due to an increase of storm events. The third phase is characterized by a return to a closed lagoon during the Medieval Warm Period (from 1100 to 1690 Cal AD). The fourth phase dated from 1690 to 1760 Cal AD coincide with "the Little Ice Age" and is marked by one specific sedimentological layer attributed to a marine submersion event. This layer could be associated to the 1693 tsunami event in southern Italy or an increase of extreme storm events. The fifth phase covering the last 250 years present a reclosing of the lagoon.

1 Introduction

Coastal storms or tsunamis are among the most dangerous events that caused significant human and economic losses along coastal regions (Seisdedos et al., 2013). One of the strongest destructive and dangerous recorded meteorological event was that of the hurricane Katrina in Florida in United States in 2005. It engenders more than $100 billion of damages, killed around 2000 people and touched 90000 square miles of the United States (Phadke, 2005). The 2004 Sumatra tsunami was consecutive to a mega-earthquake with M_w9.2. This tsunami generated high waves up to 30 meters and induced 250.000 dead peoples (Lay et al., 2005). This tsunami was considered by many Indonesian peoples as the most disastrous event compared to other major

https://doi.org/10.5194/nhess-2020-311
Preprint. Discussion started: 3 November 2020


Natural Hazards and Earth System Sciences Discussions

past catastrophic events that had occurred in 1797 and 1833 (Natawidjaja et al., 2006).

The Mediterranean basin is defined as an "Hotspot" of the climate change (Lionello and Scarascia, 2018 ; Pausas and Millán, 2019). According to the IPCC (2014), the coastal erosion and submersion is one of the results of an elevation of sea-level due to the global warming. The Mediterranean Sea surface temperature has increased by almost 1°C since 1980 and expected to rise further by 2.5 °C in the next seventy years (Jacqueline Karas, 2006). In this context, the Mediterranean coastal zones will be probably more vulnerable to the climatic extreme events (storms and medicanes), and more exposed to coastal erosion processes and flooding (Seisdedos et al., 2013). The Mediterranean basin is also characterized by a high seismic activity due to its geographical position between the Eurasian and African plates (Papadopoulos and Fokaefs, 2005; Papadopoulos and Baskoutas, 2009). The earthquake of the 21st of May 2003 that happened in the Western Mediterranean Sub-basin precisely in Boumerdes (Algeria) with a magnitude of about 6.8 has generated a tsunami (Belazougui, 2008). The low wave generated has a height < 25 cm and propagated from the Algerian coast toward the Murcia Province. These waves have not caused any evident damages (Álvarez-Gómez and Gonzalez, 2011). However, in the Eastern Mediterranean sub-basin, the Crete earthquake (21st July 365 AD) induced a tsunami that propagated across the region to reach Alexandria and has hit the Cretan coast causing extensive damage (François, 1984).

Due to the absence of data covering a sufficiently long time period, the recent instrumental data, and textual archive on extreme events (storm and tsunami) in Tunisia do not allow us to determinate any evolution in time. According to Morton et al. (2007); Dezileau et al. (2011); Sabatier et al. (2012) and Degeai et al. (2015), these sedimentary inputs coming from the sea during marine submersions, will permit the study of these extremes events over a longer period of time. A historical catalog of tsunamis and storms is being built in the Mediterranean region (e.g., Goldfinger et al., 2013), but there is a very few information on the Tunisian coasts. The aim of this study is to reconstruct the evolution of Ghar el Melh lagoon and to identify the different extreme events (storms or tsunamis) using a multi-proxy analysis based on geochemical and sedimentological approaches of two sediment cores GEM3 and GEM4 collected from the lagoon of the Ghar el Melh in the North-western part of the Gulf of Tunis.

2 The study site of Ghar El Melh

2.1 Geological Sitting

This work focuses on the Ghar el Melh lagoon situated in the Northeast of Tunisia. This lagoon is called also "the Porto Farina". It has an elliptic shape and approximately a surface of 28.5 km^2. Its average depth is about ~0.8 m (Romdhane, 1985; SCET-ERI, 2000; Moussa et al., 2005). This lagoon is directly limited in the north side by a mountain range called "Jbel Nadhour" (325 m). This mountain is composed of a marine Pliocene material (Figure 1). The lagoon is bordered by marshy grounds to the west and to the south. While in the eastern side, it was separated from the sea by a sandy barrier, with a local opening (El Boughaz) allowing a permanent hydraulic communication (Oueslati et al., 2006). According to Paskoff (1994),

https://doi.org/10.5194/nhess-2020-311
Preprint. Discussion started: 3 November 2020


Natural Hazards and Earth System Sciences Discussions

the lagoon was considered as a vestigial and remaining part of the Utique Sea that was formed during the last postglacial transgression since 6000 years ago. Progressively, this small gulf has been disconnected from the Utique Sea, due to Medjerda fluvial deposits (Paskoff and Trousset, 1992). This caused a progressive reshaping of the lagoon to its present morphology, which could be attributed to an association of the shape of the coastline and alluvium deposition from the Medjerda River (Moussa et al., 2005).

2.2 Climatological and hydrological settings

The Northeast of Tunisia is characterized by a typical Mediterranean climate with hot arid summer and rainy winter characterized generally by heavy rainfall periods and floods. The rainfall mean annual in the lower valley of the Medjerda is around 500 mm.yr-1 (Oueslati, 2004). Furthermore, in this study area, the rainfall rate is very variable. The mean winter temperatures are around ~11 °C. The highest precipitation occurred mainly between November and December with an average of 248 mm (INS, 2001). The monthly average values sometimes exceed 100 mm (Beni Atta Station in December) and never fall below 60 mm (MEAT, 2001). The high temperatures are observed in August with mean values of ~27 °C. In other hand, the salinity in the lagoon depends on the hydrological balance and varies from 36 g/l in winter to 51 g/l in summer due to the highest evaporation rate 1450 mm/year (Added, 2001; Moussa et al., 2005; Oueslati et al., 2006).

3 Material and methods

3.1 Sampling location and sediment samples

Two piston cores were collected in 2012 in the Northeast of Ghar el Melh lagoon. These cores are 126 cm (GEM4) and 98 cm (GEM3) length (Figure 1). They were manually sampled according a transect East West into the lagoon (~200m from the sandy barrier for GEM3 and ~400m for GEM4). In the laboratory, the two cores GEM4 and GEM3 were divided, photographed, and described in detail. Before granulometric and geochemical analyses, the cores were split into 1 cm vertical sections. Moreover, 29 surface sediment samples were collected from the Medejerda watershed to the sandy barrier of Ghar el Melh to assess the origin of the lagoon sediment: (i) 6 samples comes from the Medjerda River (Gr01 to Gr06), (ii) 12 samples from different small affluents located in the northern and western part of the lagoon (from Gr07 to Gr18) and (iii) 11 samples from the sandy barrier (Gr19 to Gr29) (Figure 1). For all samples, the position was registered using a GPS "GPSmap 60, Garmin". In the laboratory, granulometric and geochemical analysis were performed on these surface samples.

3.2 Sedimentology and geochemistry analysis

To determinate the distribution of grain size a particle Size analysis was adopted by using a Beckman Coulter© LS 13 320 (Geosciences Montpellier). Due to the high concentration of shells fragments (>200 µm), every sample was sieved at 150 µm before analyses. An ultrasounds were used to avoid particles flocculation, after the entrance of sediments into the fluid module

https://doi.org/10.5194/nhess-2020-311
Preprint. Discussion started: 3 November 2020


Natural Hazards and Earth System Sciences Discussions

of the granulometric. We used an XRF core scanner Niton XL3t to analyzed sediment cores and surface samples by X-ray fluorescence (XRF). In order to avoid desiccation of the sediment and contamination of the XRF measurement unit, samples had to be covered with an Ultralean film. The geochemical analysis from XRF measurements was executed in the mining type ModCF proline mode. These semi-quantitative elemental measurements were performed along with the sediment core every 1 cm. The elemental concentrations obtained are expressed in ppm or percentage values. To evaluate the analytical error and the precision of measurement, international powder standards (NIST2702 and NIST2781) were adopted, it was between 10 and 25% for the "Si", and lower than 5% for the "Ca", "Sr", "Ti", "Fe", "Zn", "Ba", and "Rb", and between 5 and 10% for the "Pb", "Zr".

3.3 Chronological framework

To determinate the chronology of the two cores GEM4 and GEM3, an accelerator Mass Spectrometry (AMS) ^{14}C dates on only one mollusk species (Cerastoderma glaucum) associated with the using of ^{210}Pb and ^{137}Cs measurements were adopted. In fact, the ^{137}Cs and ^{210}Pbex activities analysis was measured by gamma spectrometry using a CANBERRA Broad Energy Ge (BEGe) detector on fine sediment (fraction < 150 µm). The $^{210}Pb_{ex}$ dating is founded on the determination of the ^{210}Pb excess activities preserved in the sediment of cores. The utilize of this natural radionuclide ^{210}Pb to indicate sedimentation rate is now a well-established technique (Goldberg, 1963; Krishnaswamy et al., 1971a; Robbins and Edgington, 1975). The dating of ^{137}Cs was released following the procedure of Robbins and Edgington (1975).

The ^{14}C analysis was conducted at the labratoire de Mesure C14 (LMC14) on the ARTEMIS accelerator in the French CEA institute (Atomic Energy Commission) at Saclay, France. These ^{14}C analyses were realized with the classical procedure illustrated by Tisnérat-Laborde et al., 2001. The radiocarbon ages were transformed into calendar ages utilizing the Marine 13 curve (Reimer et al., 2009). The radiocarbon ages of marine and lagoonal organisms are generally ancient than the atmospheric 14C ages and have been calculated and modified by subtracting the « reservoir age » (Zoppi et al., 2001; Siani et al., 2001; Reimer and McCormac, 2002; Sabatier et al., 2010 ; Dezileau et al., 2016).

4 Results

4.1 Characterization of different detrital surface sources

To better characterize the geochemistry of sediment sources in the lagoon of Ghar el Melh, we analyzed the geochemical results obtained for the sediment samples with a statistical method called principal component analysis (PCA) (Figure 2). This statistical approach was applied to distinguish the different surface sediment sources in relationship with the geochemical processes or the chemical elements proprieties. The PCA dataset input consists of 29 samples that were analyzed for their major and trace elements ("Ca", "Sr", "Fe", "Rb", "Ba", "Ti", "Mn", "Zn" and "Si") and were presented as elemental concentrations (9 variables). The two first factorial factors represented in the PCA diagram present (Figure 2) 72.25% of the

https://doi.org/10.5194/nhess-2020-311
Preprint. Discussion started: 3 November 2020


Natural Hazards and Earth System Sciences Discussions

entire variance of the dataset. The factor 1 accounts for 61.12% of the entire variance. Factor number 1 is marked by a positive loading for terrigenous elements "Rb", "Ti", "Ba", "Mn", "Fe", and "Zn". Whereas the "Ca" and "Sr" present a modest positive loading and are inserted in factor 1. Factor 2 represents 11.13% of the global variance. It indicates positive loading for "Si", "Mn", "Ti", "Ba", "Zn", "Rb", and "Fe", whereas "Sr" and "Ca" have negative loadings. Based on these statistical analyses of geochemical data, three distinct sources of sediments were identified (Figure 2): (i) Terrigenous or Alluvial source ("Mn", "Fe", "Zn", "Ba", "Rb") mainly discharged by rivers during floods. (ii) Marine source "Si" such as sands coming from the sandy barrier coastal during marine submersion; (iii) and a biogenic origin ("Sr" and "Ca").

According to this funding, the sedimentation in the lagoon of the Ghar el Melh is generally manifested by marine and terrestrial inputs. Indeed, the geographic distribution (Figure 3) of granulometric results indicates that the high percentage of coarse sediments "sands" (% >75%) are from the sandy barrier, whereas, sediments of the Medjerda watershed are distinguished by a very high percentage of fine sediments (Silt and Clay). Medjerda River and the affluent around it constitute the main origins of fine fractions (Clay) in the Ghar el Melh lagoon. The mapping of terrigenous elements such as Silicon, Titanium, and Iron contents in surface sediments confirm this distinction of detrital origins around the Ghar el Melh lagoon. High "Si" values (>110000 ppm) distinguish especially the sandy barrier. Moreover, the highest contents of Titanium "Ti" (> 1400 ppm) and Iron "Fe" (> 17500 ppm) are retrieved in sediment from the watershed of the Medjerda (Figure 4). This difference in the origin of the terrigenous inputs in Ghar el Melh lagoon could be explained by the fact that, during floods events, finer sediments are coming from the Medejerda watershed whereas, at the time of marine storms, coarse marine sand inputs are from the barrier.

Therefore, the geochemical analysis confirms the results of granulometric analysis by showing that the sedimentation of this lagoon was controlled by marine and continental contributions.

4.2 Downcore results

4.2.1 Age model

The chronology of the GEM3 and GEM4 cores has been established using the ^{14}C dates and also the ^{137}Cs and ^{210}Pb measurements on monospecific mollusk shell samples and bulk sediments, respectively. In the uppermost 30 cm of the two cores, the measured $^{210}Pb_{ex}$ values range in GEM3 from 287.47 to 2.29 $mBqg^{-1}$ and f in GEM4 from 253.67 to 1.01 $mBqg^{-1}$. In general, the down-core distribution of ^{210}Pb excess values follows a relatively exponential decrease with depth. Based on a model Constant Flux, Constant Sedimentation Rate (CFCS) (applicated by Goldberg, 1963; Krishnaswamy et al., 1971), the ^{210}Pb data determinate a sedimentation rate of 0.7 mm $year^{-1}$ for GEM3 and 0.6 mm $year^{-1}$for GEM4. The distribution profile of ^{137}Cs activity shows for the first 10 cm (Figure 5) a maximum value at 3.5 cm in GEM3 and 3 cm in GEM4. This can represent the period of the utmost radionuclide fallout in the Northern Hemisphere which was related to the weapons atomic peak testing in 1963. The ^{137}Cs obtained sedimentation rate is about ~0.7 mm $year^{-1}$ for the GEM3 which is slightly higher than that obtained for GEM4 (0.6 mm $year^{-1}$; Figure 6). The distribution profile of the total "Pb" shows that the beginning of the industrial pollution in 1892 (Latour, 2019) is situated at 9 cm, indicating a sedimentation rate of about 0.75 mm $year^{-1}$ for

https://doi.org/10.5194/nhess-2020-311
Preprint. Discussion started: 3 November 2020


Natural Hazards and Earth System Sciences Discussions

both cores (Figure 6). Thereby, sedimentation rate of the GEM3 core calculated using the ^{137}Cs, ^{210}Pb and total "Pb" show similar values around 0.75 mm year^{-1}, which are slightly higher than that for GEM4 (mean value of around of ~0.6 mm year^{-1}). The conventional AMS-^{14}C measurements were performed using mollusk shells (*Cerastoderma glaucum*) on eight control points for GEM3 (Table 1) and seven ones for the GEM4 (Table 2). Taking into account both the radiocarbon and $^{210}Pb_{ex}$ dates, the local ^{14}C reservoir age in the Ghar el Melh lagoon was determined. According to the method of Sabatier et al. (2010), the evaluation of the modern ^{14}C reservoir age was conducted by comparing an age obtained from ^{137}Cs and ^{210}Pb data, and from geochemical analysis of mining-contaminated lagoonal sediments with an AMS^{14}C age of a pre-bomb mollusk shell.

According to Reimer et al. (2013), the Sea surface reservoir age R(t) for the recent shell (SacA44506) was measured by subtracting the atmospheric ^{14}C value determined for the historical date 1845 AD (114±8 ^{14}C years) from the measured apparent ^{14}C ages of the shell (450±30 ^{14}C years, Table 3). This determines an R(t) value of 363 years. The deviance from the total mean reservoir age (ΔR) is then calculated by subtracting the marine model age value obtained for 1845 AD (453±23 ^{14}C years) from the measured apparent ^{14}C age of the mollusk (450±30 ^{14}C years; Table 3). The calculated ΔR of around 2 years (Table 3) is thus, adopted. The reservoir age of this lagoon is similar to the marine reservoir age. Finally, the age model of GEM3 and GEM4 cores was established by using the OxCal 4 on ^{14}C ages and $^{210}Pb_{ex}$ /^{137}Cs average sedimentation rates. The ^{14}C mean sedimentation rate calculated is then about ~2.5mm year^{-1} (Figure 7A).

As the GEM4 indicates a level of erosion or inactive deposition process named "a Condensed area" observed from 59 to 72 cm (between 0 and 1000 Cal AD/BC), which would instigate an error in the obtained age model (Figure 7B), the discussion will be focused only on the ages estimated from GEM3 core. The age correction has been obtained by the correlation between the Strontium profile of the two cores GEM3 and GEM4.

4.2.2 Lithological, granulometric and geochemical studies of GEM3 and GEM4 cores

Two sedimentary cores were collected in the northeastern of Ghar el Melh lagoon. They contain fine sediments (clay and silt) interbedded with coarse-grained layers formed by mollusk fragments and siliciclastic sand. The sedimentary succession in the GEM3 core is very comparable to that presented in GEM4 (Figure 8). Whereas, the thickness of sandy layers is slightly different between the two cores. This could be attributed to the geographical position of core GEM3, which is closer to the sandy barrier (~200m) than core GEM4 (~400m).

The GEM3 and GEM4 sediment cores of 97 and 126 cm long show visual variation in the sediment composition. Lithological description of these two cores highlighted three distinct sedimentary facies (Figure 8): The Basal unit (1), situated between 126 - 67 cm in GEM4 and between 97 - 85 cm in GEM3, is composed generally of a lighter grey silty layer and shells. At the base (the last 3 cm for the GEM3 and the last 13 cm for the GEM4) the lithological composition of this unit is characterized by a very thin fine sandy layer. For the GEM3, the transition between unit (1) to unit (2) is defined by a sharp contact; The Middle Unit (2), situated between 85 -63 cm in GEM3 and between 66 – 60 cm in GEM4, is typically composed of a lighter

https://doi.org/10.5194/nhess-2020-311
Preprint. Discussion started: 3 November 2020


Natural Hazards and Earth System Sciences Discussions

grey sandy layer with a combination of shell fragments and sands; The Upper unit (3): <60 cm in GEM4 and <63 cm in GEM3,is composed mainly of organic-rich clay and shells with the intercalation of a sandy layer situated between 36 and 26 cm in GEM3 and between 30 and 24 cm in GEM4 (Figure 8). This sand layer is usually characterized by coarse sediments with light colours and also dominated by shell fragments. This coarse grain size layer intercalated in the mud sediments indicates an "energetic" event, relative to the background sedimentation. It is probably linked to washover event and marine incursion during an intense event such as a storm or tsunami.

The granulometric analysis shows that the silty clay is the most abundant fraction in our sediment cores (Figure 8). However, sand is dominant at two levels. The first layer occurred between 86 and 64 cm in GEM3 and between 60 and 65 cm in GEM4 whereas the second one is observed from 35 to 26 cm in GEM3 and from 30 to 24 cm in GEM4. These two layers are characterized by the dominance of a sandy quartz material and shell fragments.

The geochemical analysis of GEM3 and GEM4 cores performed using an XRF core scanner, have detected 21 chemical elements ("Zr", "Si", "Sr", "Rb", "Th", "Pb", "Zn", "Cu", "Ni", "Fe", "Mn", "V", "Ti", "Sc", "Ca", "K", "S", "Ba", "Cs", "Te", and "Sn") above the limit of detection. Among these elements, we choose to represent in Figure 8 only those with a significant down core variation which are "Si", "Ca", "Sr", and "Ti". The Silicon "Si" will represent the marine geochemical pole, while "Ti" represents the terrigenous one. According to the granulometric and geochemical results of surface samples, the "Ti" is associated with the silt-clay fraction whereas the "Si" is associated with the sandy fraction. Furthermore, the highest Strontium "Sr" and Calcium "Ca" values in the two cores are found to be related with the silt-clay fraction between 62 and 33 cm in GEM3 and between 60 and 30 cm in GEM4. The "Sr" and "Ca" represent a biogenic geochemical pole linked to marine shells. These results are in agreement with those acquired by the statistical method (PCA) in surface samples.

5 Discussion

According to our granulometric, geochemical results, we can divide the Late Holocene lagoonal history into five phases that record the connection between the lagoon and the sea in relation to the sandy barriers evolution. The different phases can be described as follow:

The first phase, dated from -275 to 200 Cal AD, is marked by a high percentage of fine sediments (about 70 % of Silt) (Figure 9). Our geochemical results show a relatively high concentration of terrigenous elements "Ti" (around 250 ppm) and "Fe" (around 2500 ppm). This predominance of the fine fraction, rich in Ti and Fe, means that the lagoon is filled in sediments coming from the Medjerda River. The presence of fine material suggests that the hydrodynamic current in the lagoon is low, we have a protected lagoon with a sandy barrier well-constructed. This accumulation of fine sediment could also indicates a higher contribution of sediments from Medjerda River. Indeed, this interval corresponds to a more humid phase (Roman Climatic Optimum) characterized in Garaet el Ichkel (North of Tunisia) by a stabilization phase of vegetation (Stevenson et al., 1993).

https://doi.org/10.5194/nhess-2020-311
Preprint. Discussion started: 3 November 2020


Natural Hazards and Earth System Sciences Discussions

The second phase has started at 200 Cal AD and finished at 1100 Cal AD. Our granulometric and geochemical results demonstrate that the sedimentation of Ghar el Melh lagoon during this period was mainly controlled by a marine contribution. This phase is marked by a decrease in the percentage of silt, and a rise in the percentage of sand (about 80 %). This time interval shows also the presence of a high amount of Silicon (Si >100000 ppm) (Figure 9) which stipulate an enhance in the sandy material supply. The decrease in the silty-clay fraction (10%) is can be related to a dilution by high marine inputs. The dominance of coarse sediment, rich in Si, could be explained by a weakening of the sandy barrier due to an increase of storm events. Degeai et al. (2015) and Sabatier et al. (2012) have clearly recorded a period of higher storm activity from 400 to 800 cal yr AD in the occidental part of the Mediterranean area. This period named Dark Age Cold Period coincides with the North Atlantic cooling phase known as Bond Event 1 (Bond et al., 2001). Dezileau et al. (2011) and Sabatier et al. (2012) have demonstrated that intervals of an enhance in storm activity in the Western Mediterranean area seem to be well related to the cold periods of the Holocene. During these cold periods, the sea ice was prolonged over the North Atlantic basin southward especially during winter (Lamb, 1995). Dezileau et al. (2011, 2016) hypothesized that this extends propose a rise in thermal gradient, leading to an enhanced lower tropospheric baroclinicity over a large Central European-Mediterranean domain. This mechanism related to a southward movement of storm track suggests an enhance of storm activity in the Western Mediterranean Sea, in accordance with simulation (Raible et al., 2007).

The third phase, dated from 1100 to 1690 Cal AD, is marked by a decrease of sandy material while the highest percentage of clay (about 30%) (Figure 9) of the whole record are observed. This kind of sedimentation is typically associated with processes of decantation in the lagoon (Liu and Fearn, 2000; Donnelly et al., 2004). Geochemical results determinate an enhance in the concentration of terrigenous elements “Ti” (around 400 ppm) and “Fe” (around 3500 ppm) (Figure 9) during this interval. This increase in the silty-clay fraction is probably due to a decrease of storm activity and/or an increase of fine sediments transported into the lagoon by rivers during periods of higher runoff. During this third phase, we have a protected lagoon again with a sandy barrier well-constructed.

The fourth phase has started at 1690 Cal AD and finished at 1760 Cal AD. This phase was characterized by a high deposition of sand, about 75 % of the total sediment (Figure 9), indicating an opening of the lagoon (Figure 10). This time interval was characterized by a sudden decrease of “Sr” (around 200 ppm) and “Ca” (around 55000 ppm) concentrations (Figure 9). The presence of coarse sediments can be explained by a higher marine influence. Interestingly, this coarse-grained layer is recorded in both cores (from 26 to 35 cm for GEM3 and from 24 to 30 cm for GEM4) collected at 200 m and 400 m from the sandy barrier respectively (Figure 10). Do we have had a major event? The relationship between the intensity of a sea extreme event (storm or tsunami) and the grain size of the overwash sand accumulated in the lagoon is very complex (Dezileau et al., 2011). Whereas, a positive relationship has been proved between storm-surge height, storm intensity, and the grain size of sands. Donnelly et al. (2001) revealed that outstandingly higher storm surges has been caused by historic and recent major hurricanes over the Atlantic coast than winter storms and minor hurricanes and demonstrated during the past several centuries, that only the major hurricanes left a regionally consistent and stratigraphically distinct record of overwash sand layers in the deposits of

https://doi.org/10.5194/nhess-2020-311
Preprint. Discussion started: 3 November 2020


Natural Hazards and Earth System Sciences Discussions

the coastal marshes. Thus, this period could be a sign of an enhance of intense storm activity. Indeed, this interval corresponds to the historic period called "Little Ice Age" (LIA) which coincides with the North Atlantic cooling phase known as Bond Event 0 (Bond et al., 2001). (Dezileau et al., 2011)); (Sabatier et al., 2012)); (Dezileau et al., 2016)) and (Degeai et al., 2015)) have clearly recorded a period of higher storm activity between 1400 and 1800 cal yr AD in the occidental region of the Mediterranean Sea. This sand deposit could also be associated to a tsunami deposit, a tsunami causing a marine submersion and an opening of the sandy barrier. This period is in line with the documented Sicilian tsunami that occurred in 1693 CE. Due to its geographic position nearby to Sicilian coast, we thought that probably, Tunisian coast and therefore Ghar el Melh lagoon can be sensitive to the 1693 tsunami. The sedimentary characteristics of tsunamis or storms deposits are almost similar ((Hawkes et al., 2007); Morton et al., 2007; Kortekaas and Dawson, 2007; Mamo et al., 2009). Regarding the diagnostic characteristics of storm or tsunami deposits, several studies have pointed out many hypotheses and determinate that their distinctions are very controversial (Tappin, 2007; Engel and Brückner, 2011; Sakuna-Schwartz et al., 2015). Considering the available data, the hypothesis of tsunami or storm origin for this recorded extreme event remains open. Deciphering the origin of this event requires further investigations, such a modeling of tsunami wave propagation for example.

The fifth phase dated from 1760 to 2012 Cal AD, is characterized by fine sediments (Figure 9). This fifth phase shows a protected lagoon (Figure 10) and suggesting that no catastrophic intense sea events have struck Gar El Melh lagoon during this last phase.

6 Conclusion

To identify the paleo-extreme events (storms or tsunamis) and to reconstruct the paleo-evolution of the lagoon of the Ghar el Melh, in the Northeast of Tunisia, high resolution of sedimentological, geochemical and geochronological analyses were used. This approach gives information about the paleoenvironmental changes of Ghar el Melh lagoon and paleo-extreme events since 2300 years. Five phases have been identified: The first phase (from -275 to 200 Cal AD) indicates a protected lagoon. The second phase dated from 200 to 1100 Cal AD shows an opening lagoon and more marine inputs. This period was may be associated with a more storm activity during the Dark Age Cold Period. The third phase indicates an isolated lagoon and coincides with the MWP (from 1100 to 1690 Cal AD). The fourth phase "the LIA" dated from 1690 to 1760 Cal AD and shows an opening of the lagoon again may be due to an enhance of storm activity or the occurrence of the 1693 tsunami event. The fifth phase covered the last 250 years and shows a reclosing lagoon. Even if our records allowed to detect past extreme events, it is not possible to differentiate if they are due to tsunamis or storms. Deciphering the origin of these events require further investigations.

Author contributions

All authors analyzed the results and prepared the manuscript.

https://doi.org/10.5194/nhess-2020-311
Preprint. Discussion started: 3 November 2020

280

Competing interests

All authors announce that no competing interests are present.

Acknowledgements

285 The authors would like to thank the Institute at Saclay (French Atomic Energy Commission) and specially the Laboratoire de Mesure 14C (LMC14) ARTEMIS at the CEA for the 14C analyses. We are grateful for the projects MISTRALS PALEOMEX, the PHC-UTIQUE no. 14G1002 and the MEDYNA FP7-IRSES 2014-2017, for your financial support. Also, we would like to thank Radewane Hout for his help in the achievement of some figures.

References

290 Added, A.: Biogeochemical cycles of Org-C, Tot-N and Tot-S in the sediment of the Ghar El Melh Lagoon (north of Tunisia), J. Mar. Syst., 30(1), 139–154, 2001.

Álvarez-Gómez, J. A. and Gonzalez, M.: Tsunami hazard at the Western Mediterranean Spanish coast from seismic sources, Nat. Hazards Earth Syst. Sci., 11, 227–240, doi:10.5194/nhess-11-227-2011, 2011.

Belazougui, M.: Boumerdes Algeria Earthquake of May 21, 2003 : Damage Anaysis and behavior of Beam- Colum Reinforced
295 Concerte Structures, in The 14th World Conference on Earthquake Engineering October 12-17, 2008, Beijing, China, pp. 1–8., 2008.

Bond, G., Kromer, B., Beer, J., Muscheler, R., Evans, M. N., Showers, W., Hoffmann, S., Lotti-Bond, R., Hajdas, I. and Bonani, G.: Persistent solar influence on North Atlantic climate during the Holocene, Science (80-.)., 294(5549), 2130–2136, 2001.

300 Degeai, J. P., Devillers, B., Dezileau, L., Oueslati, H. and Bony, G.: Major storm periods and climate forcing in the Western Mediterranean during the Late Holocene, Quat. Sci. Rev., 129, 37–56, doi:10.1016/j.quascirev.2015.10.009, 2015.

Dezileau, L., Sabatier, P., Blanchemanche, P., Joly, B., Swingedouw, D., Cassou, C., Castaings, J., Martinez, P. and Von Grafenstein, U.: Intense storm activity during the Little Ice Age on the French Mediterranean coast, Palaeogeogr. Palaeoclimatol. Palaeoecol., 299(1), 289–297, 2011.

305 Dezileau, L., Pérez--Ruzafa, A., Blanchemanche, P., Degeai, J. P., Raji, O., Martinez, P., Marcos, C. and Von Grafenstein, U.: Extreme storms during the last 6500 years from lagoonal sedimentary archives in the Mar Menor (SE Spain), Clim. Past, 12(6), 1389–1400, doi:10.5194/cp-12-1389-2016, 2016.

Donnelly, J. P., Roll, S., Wengren, M., Butler, J., Lederer, R. and Webb, T.: Sedimentary evidence of intense hurricane strikes from New Jersey, Geology, 29(7), 615–618, 2001.

310 Donnelly, J. P., Webb III, T., Murnane, R. and Liu, K.: Backbarrier sedimentary records of intense hurricane landfalls in the northeastern United States, Hurricanes Typhoons Past, Present. Futur., 55, 58–95, 2004.

Engel, M. and Brückner, H.: The identification of palaeo-tsunami deposits a major challenge in coastal sedimentary research,

https://doi.org/10.5194/nhess-2020-311
Preprint. Discussion started: 3 November 2020

Coastline Reports, 17, 65–80, 2011.

François, J.: Le raz de marée du 21 juillet 365.[Du cataclysme local à la catastrophe cosmique], Mézanges l'Ecole française Rome. Antiq., 96(1), 423–461, 1984.

Goldberg, E. D.: Geochronology with 210Pb, Radioact. dating, 121, 121–131, 1963.

Goldfinger, C., Morey, A. E., Black, B., Beeson, J., Nelson, C. H. and Patton, J.: Spatially limited mud turbidites on the Cascadia margin: Segmented earthquake ruptures?, Nat. Hazards Earth Syst. Sci., 13, 38, 2013.

Hawkes, A. D., Bird, M., Cowie, S., Grundy-Warr, C., Horton, B. P., Shau Hwai, A. T., Law, L., Macgregor, C., Nott, J., Ong, J. E., Rigg, J., Robinson, R., Tan-Mullins, M., Sa, T. T., Yasin, Z. and Aik, L. W.: Sediments deposited by the 2004 Indian Ocean Tsunami along the Malaysia-Thailand Peninsula, Mar. Geol., 242(1–3), 169–190, doi:10.1016/j.margeo.2007.02.017, 2007.

INS: Annuaire statistique de la Tunisie., 2001.

IPCC: Climate Change 2014 Synthesis Report., 2014.

Jacqueline Karas: Climate Change and the Mediterranean Region., 2006.

Kortekaas, S. and Dawson, A. G.: Distinguishing tsunami and storm deposits: an example from Martinhal, SW Portugal, Sediment. Geol., 200(3), 208–221, 2007.

Krishnaswamy, S., Lal, D., Martin, J. M. and Meybeck, M.: file:///C:/document bureau/figure article/refe article/hawkes 2012.txt, Earth Planet. Sci. Lett., 11(1–5), 407–414, 1971a.

Krishnaswamy, S., Lal, D., Martin, J. M. and Meybeck, M.: Geochronology of lake sediments, Earth Planet. Sci. Lett., 11(1–5), 407–414, 1971b.

Lamb, H. H.: Climate, History and the Modern World., 1995.

Latour, E. de F. de: L'industrie minière en tunisie (1892-1937)., 2019.

Lay, T., Kanamori, H., Ammon, C. J., Nettles, M., Ward, S. N. and Aster, R.: The great Sumatra-Andaman earthquake of 26 December 2004, Science (80-.)., 88(1), 11–12, doi:10.1126/science.1118950, 2005.

Lionello, P. and Scarascia, L.: The relation between climate change in the Mediterranean region and global warming, Reg. Environ. Chang., 18(5), 1481–1493, 2018.

Liu, K. and Fearn, M. L.: Reconstruction of prehistoric landfall frequencies of catastrophic hurricanes in northwestern Florida from lake sediment records, Quat. Res., 54(2), 238–245, 2000.

Mamo, B., Strotz, L. and Dominey-Howes, D.: Tsunami sediments and their foraminiferal assemblages, Earth-Science Rev., 96(4), 263–278, 2009.

MEAT: Communication Initiale de la Tunisie à la Convention Cadre des Nations Unies sur les changements climatiques., 2001.

Morton, R. A., Gelfenbaum, G. and Jaffe, B. E.: Physical criteria for distinguishing sandy tsunami and storm deposits using modern examples, Sediment. Geol., 200(3), 184–207, 2007.

Moussa, M., Baccar, L. and Ben Khemis, R.: La lagune de Ghar El Melh: Diagnostic écologique et perspectives

https://doi.org/10.5194/nhess-2020-311
Preprint. Discussion started: 3 November 2020

d'aménagement hydraulique, Rev. des Sci. l'eau, 18, 13–26, 2005.

Natawidjaja, D. H., Sieh, K., Chlieh, M., Galetzka, J., Suwargadi, B. W., Cheng, H., Edwards, R. L., Avouac, J. P. and Ward, S. N.: Source parameters of the great Sumatran megathrust earthquakes of 1797 and 1833 inferred from coral microatolls, J. Geophys. Res. Solid Earth, 111(6), 1–37, doi:10.1029/2005JB004025, 2006.

Oueslati, A.: Littoral et aménagement en Tunisie: des enseignements de l'expérience du vingtième siècle et de l'approche géoarchéologique à l'enquête prospective, Publications de la Faculté des Sciences Humaines et Sociales., 2004.

Oueslati, W., Added, A. and Adeljaouad, S.: Acide Volatile Sulfides" et "simultaneously extracted metals dans les sédiments des carottes prélevées dans la lagune de Ghar El Melh, Nord Tunisien, Rev. Méditerr. Env., 1, 15–18, 2006.

Papadopoulos, G. A. and Baskoutas, I.: New tool for the spatio-temporal variation analysis of seismic parameters, Nat. Hazards Earth Syst. Sci., 9, 859–864, 2009.

Papadopoulos, G. A. and Fokaefs, A.: Strong tsunamis in the mediterranean sea : A re-evaluation, J. Earthq. Technol., 42(4), 159–170, 2005.

Paskoff, R.: Le delta de la Medjerda (Tunisie) depuis l'Antiquité, Etud. Rurales, 15-29file:///C:/Users/Asus/Desktop/refe article/Pa, 1994.

Paskoff, R. and Trousset, P.: L'ancienne Baie d'Utique: du témoignage des textes à celui des images satellitaires, Mappemonde, 1, 30–34, 1992.

Pausas, J. G. and Millán, M. M.: Greening and Browning in a Climate Change Hotspot: The Mediterranean Basin, Bioscience, 69(2), 143–151, 2019.

Phadke, R.: Exposing Hurricane Katrina : The Scope of an Unnatural Disaster., 2005.

Raible, C. C., Yoshimori, M., Stocker, T. F. and Casty, C.: Extreme midlatitude cyclones and their implications for precipitation and wind speed extremes in simulations of the Maunder Minimum versus present day conditions, Clim. Dyn., 28(4), 409–423, 2007.

Reimer, P. J. and McCormac, F. G.: Marine Radiocarbon Reservoir Corrections for the Mediterranean and Aegean Seas, Radiocarbon, 44(01), 159–166, 2002.

Reimer, P. J., Baillie, M. G. L., Bard, E., Bayliss, A., Beck, J. W., Blackwell, P. G., Ramsey, C. B., Buck, C. E., Burr, G. S., Edwards, R. L. and others: IntCal09 and Marine09 radiocarbon age calibration curves, 0--50,000 years cal BP, Radiocarbon, 51(04), 1111–1150, 2009.

Reimer, P. J., Bard, E., Bayliss, A., Beck, J. W., Blackwell, P. G., Bronk Ramsey, C., Buck, C. E., Cheng, H., Edwards, R. L., Friedrich, M., Grootes, P. M., Guilderson, T. P., Haflidason, H., Hajdas, I., Hatté, C., Heaton, T. J., Hoffmann, D. L., Hogg, A. G., Hughen, K. A., Kaiser, K. F., Kromer, B., Manning, S. W., Niu, M., Reimer, R. W., Richards, D. A., Scott, E. M., Southon, J. R., Staff, R. A., Turney, C. S. M. and van der Plicht, J.: IntCal13 and Marine13 Radiocarbon Age Calibration Curves 0–50,000 Years cal BP, Radiocarbon, 55(4), 1869–1887, doi:10.2458/azu_js_rc.55.16947, 2013.

Robbins, J. A. and Edgington, D. N.: Determination of recent sedimentation rates in Lake Michigan using Pb-210 and Cs-137, Geochim. Cosmochim. Acta, 39(3), 285–304, 1975.

https://doi.org/10.5194/nhess-2020-311
Preprint. Discussion started: 3 November 2020

Romdhane, M. S.: Lagune de Ghar El Melh: milieu, peuplement, exploitation, Tunis (Tunisia)., 1985.

Sabatier, P., Dezileau, L., Blanchemanche, P., Siani, G., Condomines, M., Bentaleb, I. and Piquès, G.: Holocene variations of radiocarbon reservoir ages in a Mediterranean lagoonal, Radiocarbon, 52(01), 91–102, 2010.

Sabatier, P., Dezileau, L., Colin, C., Briqueu, L., Bouchette, F., Martinez, P., Siani, G., Raynal, O. and Von Grafenstein, U.: 7000years of paleostorm activity in the NW Mediterranean Sea in response to Holocene climate events, Quat. Res., 77(1), 1–11, 2012.

Sakuna-Schwartz, D., Feldens, P., Schwarzer, K., Khokiattiwong, S. and Stattegger, K.: Internal structure of event layers preserved on the Andaman Sea continental shelf, Thailand: tsunami vs. storm and flash-flood deposits, Nat. Hazards Earth Syst. Sci., 15(6), 1181–1199, 2015.

SAMAALI, H.: Etude de l'évolution de l'occupation et de l'utilisation du sol dans le delta de Mejerda par télédétection et systèmes d'informations géographiques., Université de Sfax., 2011.

Seisdedos, J., Mulas, J., González de Vallejo, L. I., Rodríguez Franco, J. A., Gracia, F. J., del Río, L. and Garrote, J.: Estudio y cartografia de los peligros naturales costeros de la region de Murcia, Bol. Geol. y Min., 124(3), 505–520, 2013.

Siani, G., Paterne, M., Michel, E., Sulpizio, R., Sbrana, A., Arnold, M. and Haddad, G.: Mediterranean Sea surface radiocarbon reservoir age changes since the last glacial maximum, Science (80-.)., 294(5548), 1917–1920, 2001.

Stevenson, A. C., Phethean, S. J. and Robinson, J. E.: The palaeosalinity and vegetational history of Garaet el Ichkeul, northwest Tunisia, The Holocene, 3(3), 201–210, 1993.

Tappin, D. R.: Sedimentary features of tsunami deposits—Their origin, recognition and discrimination: An introduction, 2007.

Tisnérat-Laborde, N., Poupeau, J. J., Tannau, J. F. and Paterne, M.: Development of a semi-automated system for routine preparation of carbonate samples, Radiocarbon, 43(2A), 299–304, 2001.

Zoppi, U., Albani, A., Ammerman, A. J., Hua, Q., Lawson, E. M. and Barbero, R. S.: Preliminary estimate of the reservoir age in the lagoon of Venice, Radiocarbon, 43(2A), 489–494, 2001.

https://doi.org/10.5194/nhess-2020-311
Preprint. Discussion started: 3 November 2020

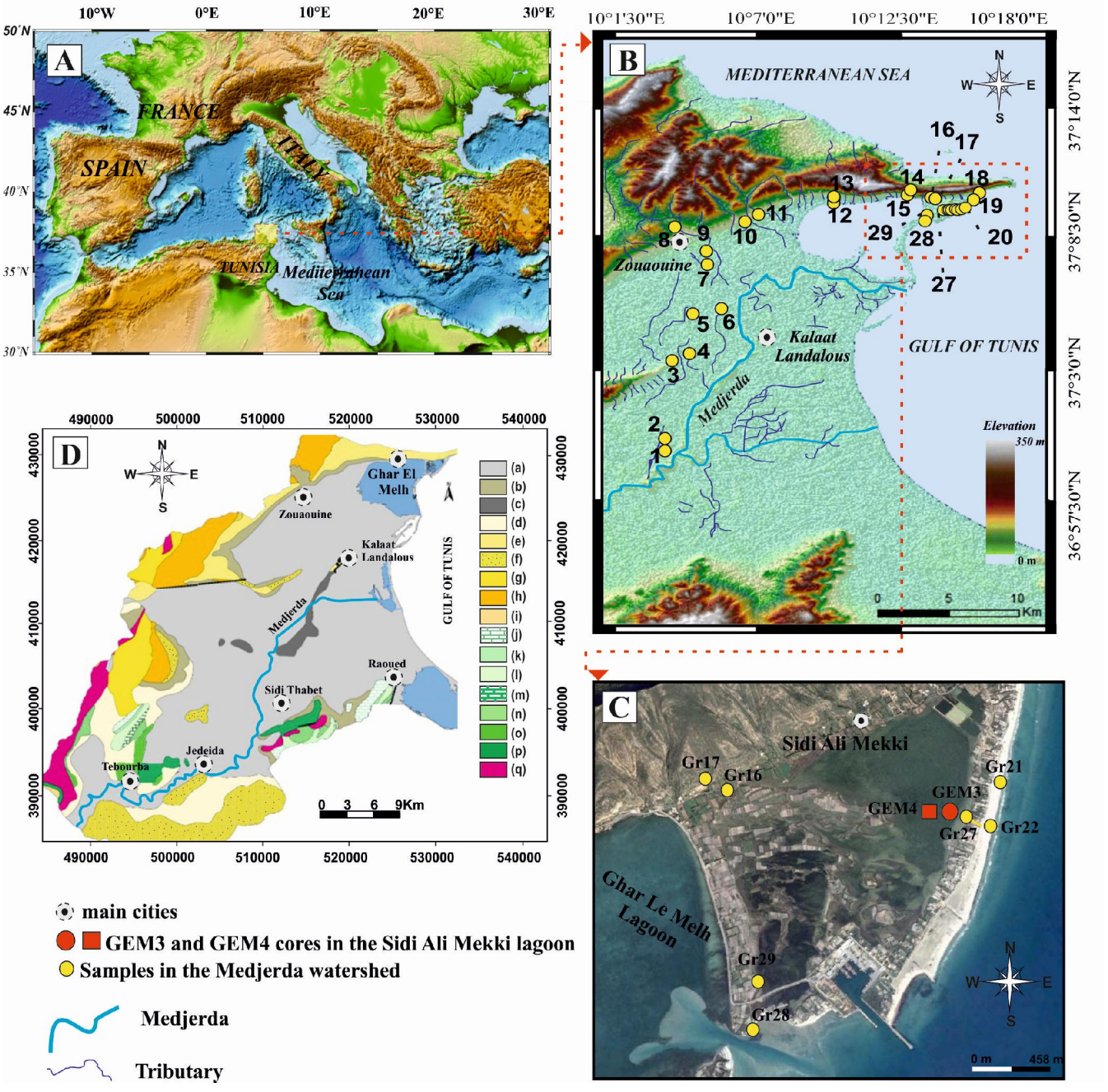

405 **Figure 1: Maps of geographic setting of the Ghar el Melh Lagoon. (A) Position of the studied region in the Northeastern Mediterranean (Ocean Data View 2013). (B) Topographic map of the lagoon and the emplacement of the different surface sediment samples preleved from the coastal plain of the Medjerda (Created by Radewane Hout using Arcgis). (C) Topographic map of the Ghar el Melh lagoon and its surroundings (e.g © Google Earth). (D) Geological maps of the Medjerda watershed (*(a) Recent alluvial soils (b) Slope deposits (c) Marine Quaternary (d) Villafranchienen (e) Pliocene (f) Continental Pliocene (g) Upper Miocene (h) Flyche*
410 *de Kchabta (i) Lower Eocene (j) Maastrichtian (k) Senonian (l) Cenomanian (m) Albian (n) Aptian (o) Barrenian (p) Valanginian-Hautrevian (q) Triassi))* **(Geological Map; Paper n ° II of Bizerte at 1/200000 modified from Samaali Hamouda, 2011).**

https://doi.org/10.5194/nhess-2020-311
Preprint. Discussion started: 3 November 2020

Natural Hazards and Earth System Sciences
Discussions

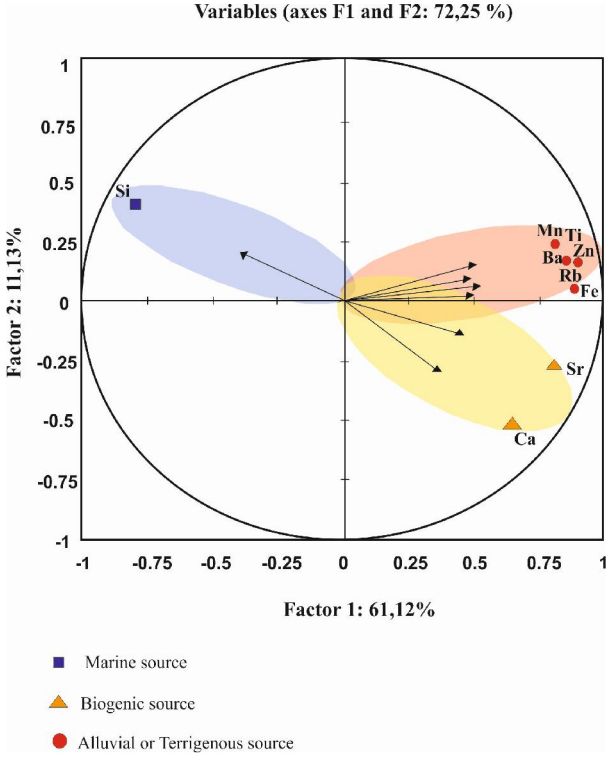

Figure 2: The different surface sediment sources from the Medjerda watershed and Ghar el Melh lagoon obtained by using a statistic model "A Principal component analysis" (PCA).

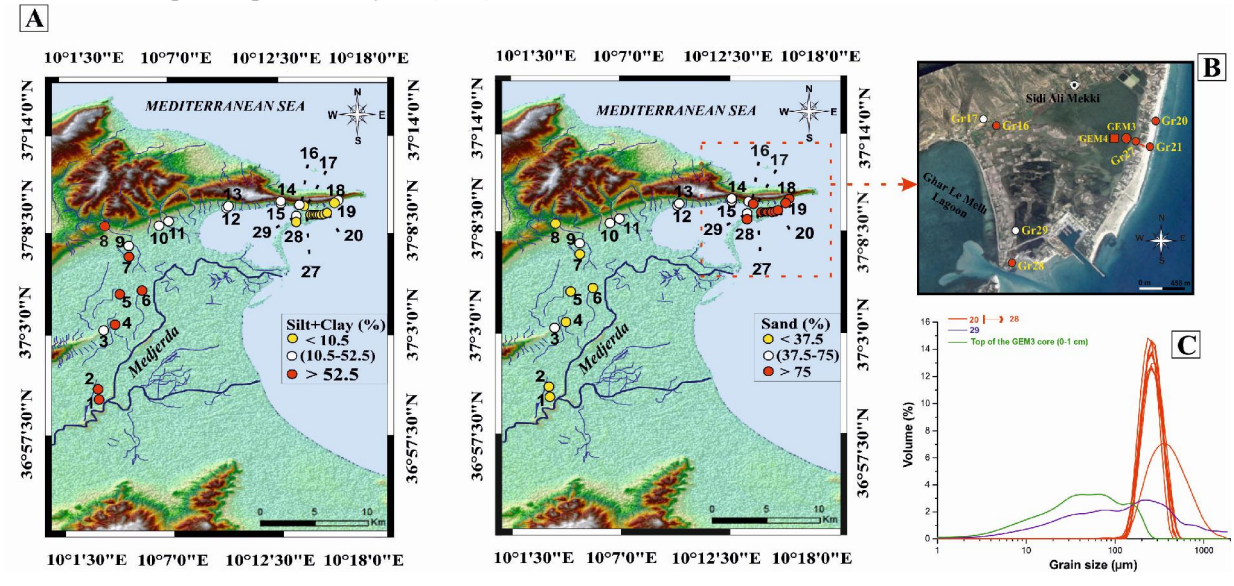

Figure 3: (3A): Topographic maps of the sand, Silt, and Clay percentage distributed in the Medjerda watershed and around the lagoon of the Ghar el Melh (Created by Radewane Hout using Arcgis). (3B) Topographic map of the two cores and the different

https://doi.org/10.5194/nhess-2020-311
Preprint. Discussion started: 3 November 2020

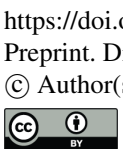

Natural Hazards and Earth System Sciences
Discussions

sediment samples collected from Ghar el Melh lagoon and its surroundings (e.g © Google Earth). (3C): Particle size distributions (ϕ < 2000 µm) of representative samples around the Ghar el Melh lagoon.

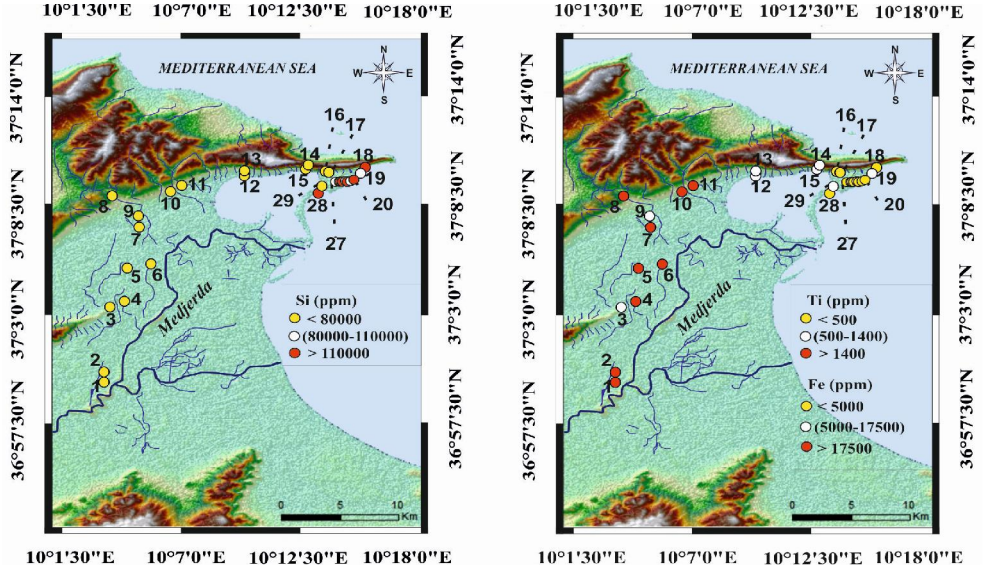

Figure 4: Topographic maps of the Iron (Fe), Titanium (Ti) and Silicon (Si) contents in the coastal plain of Medjerda and around Ghar el Melh lagoon (Created by Radewane Hout using Arcgis).

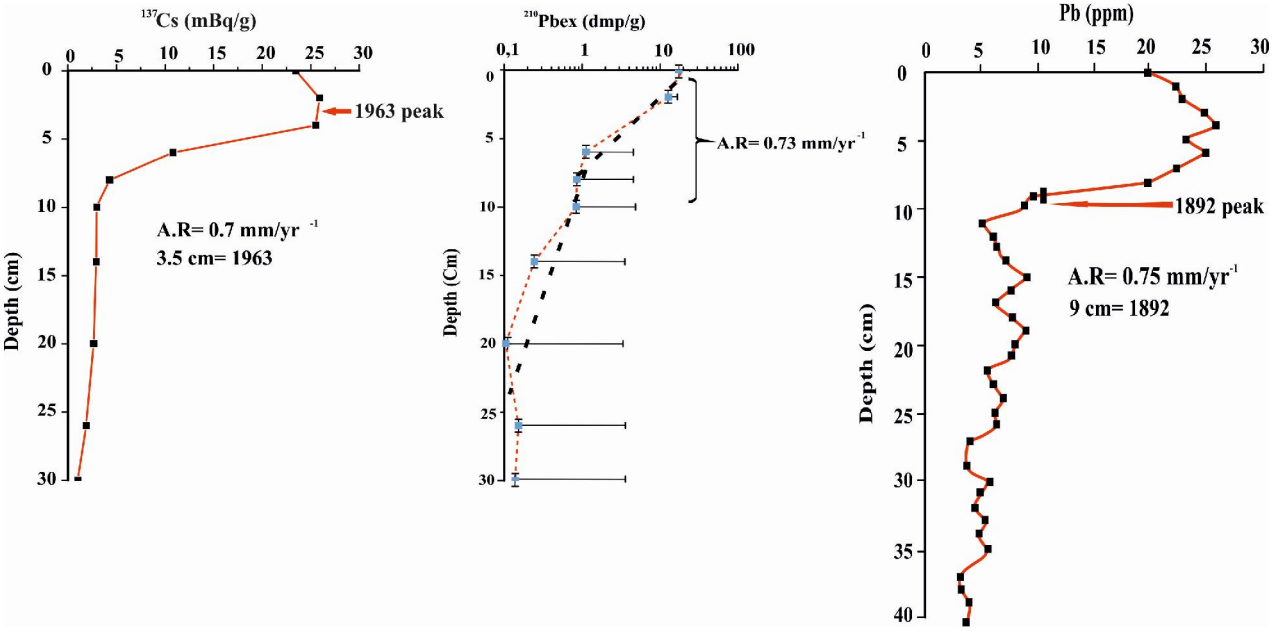

Figure 5: Distributions profile of ^{210}Pbex, Pb and ^{137}Cs vs. depth in the GEM3. The ^{210}Pb data determinate a sedimentation rate of 0.73 Mm year^{-1}. The activity depth profile Cs present a peak at 3.5 cm, indicating in accumulation rates of 0.7 mm year^{-1} for the 1963 depths.

https://doi.org/10.5194/nhess-2020-311
Preprint. Discussion started: 3 November 2020

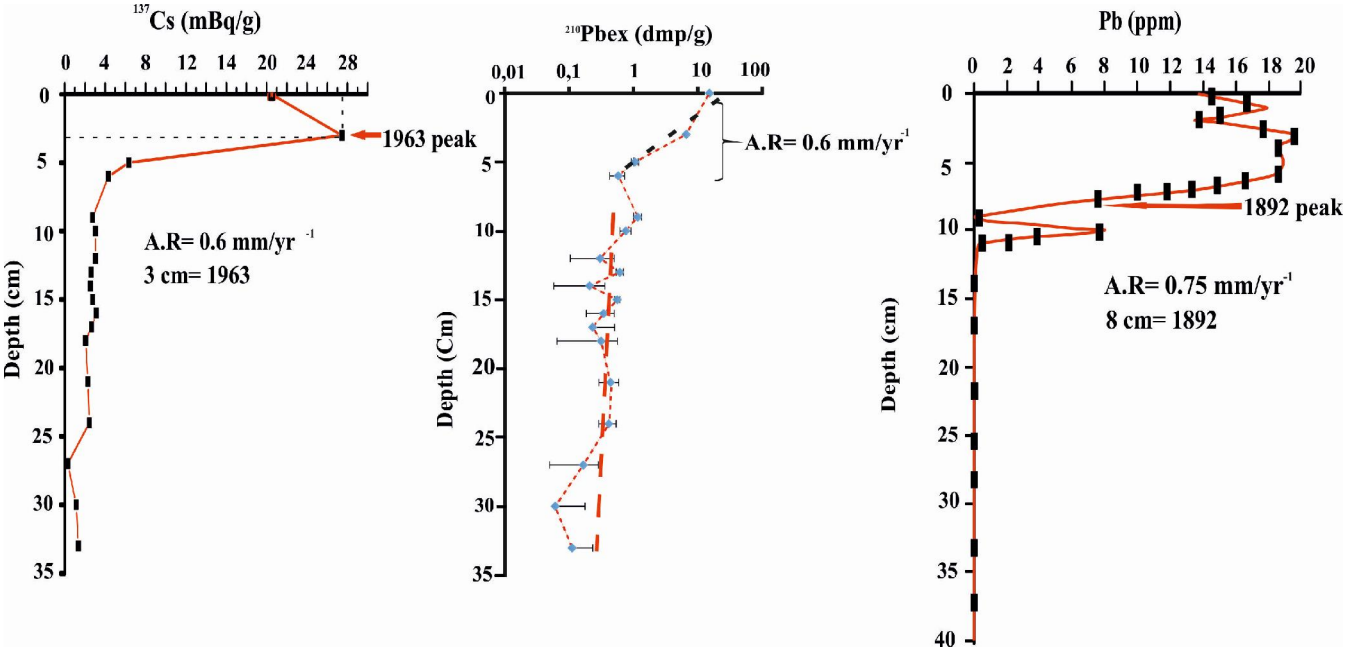

Figure 6: Distributions profile of ^{210}Pbex, Pb and ^{137}Cs vs. depth in the GEM4. The ^{210}Pb data present a sedimentation rate of 0.6 mm year-1. The activity depth profile Cs indicate a peak at 3 cm, determining in accumulation rates of 0.6 mm year^{-1} for the 1963 depths.

https://doi.org/10.5194/nhess-2020-311
Preprint. Discussion started: 3 November 2020

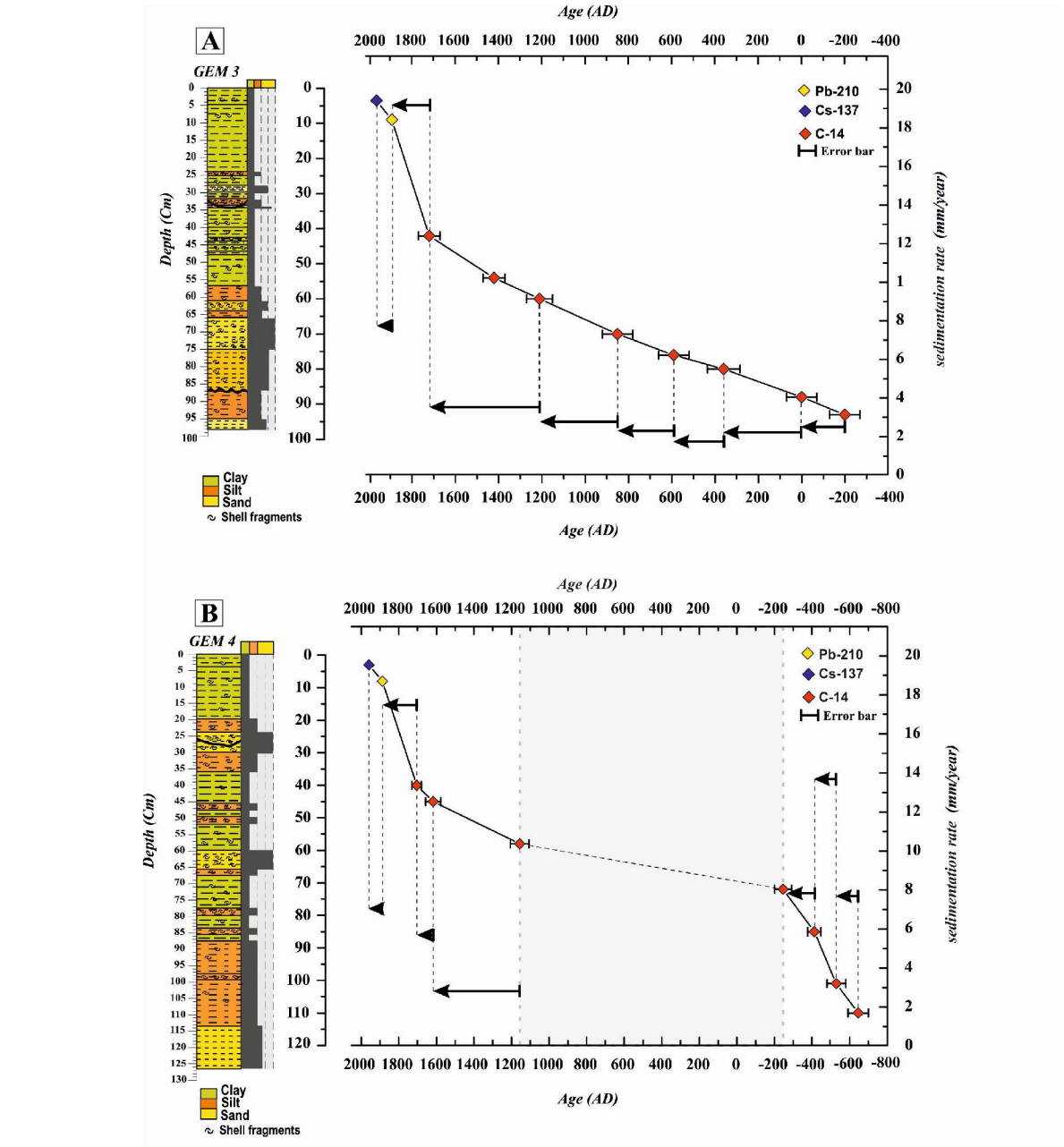

Figure 7: (7A): Sediment age-depth for the core GEM3 sampled from Ghar el Melh lagoon (Arrows: sedimentation rates variation). The OxCal 4.3 have been used to calculated the age model with 8 samples for ^{14}C dates and only one sample for each Pb and Cs dates. (7B): Sediment age-depth for the core GEM3 sampled from Ghar el Melh lagoon (Arrows: sedimentation rates variation). The OxCal 4.3 have been used to calculated the age model with 7 samples for 14C dates and only one sample for each Pb and Cs dates. The blue band determines a period of inactive deposition process or erosion so-called "a Condensed area".

https://doi.org/10.5194/nhess-2020-311
Preprint. Discussion started: 3 November 2020

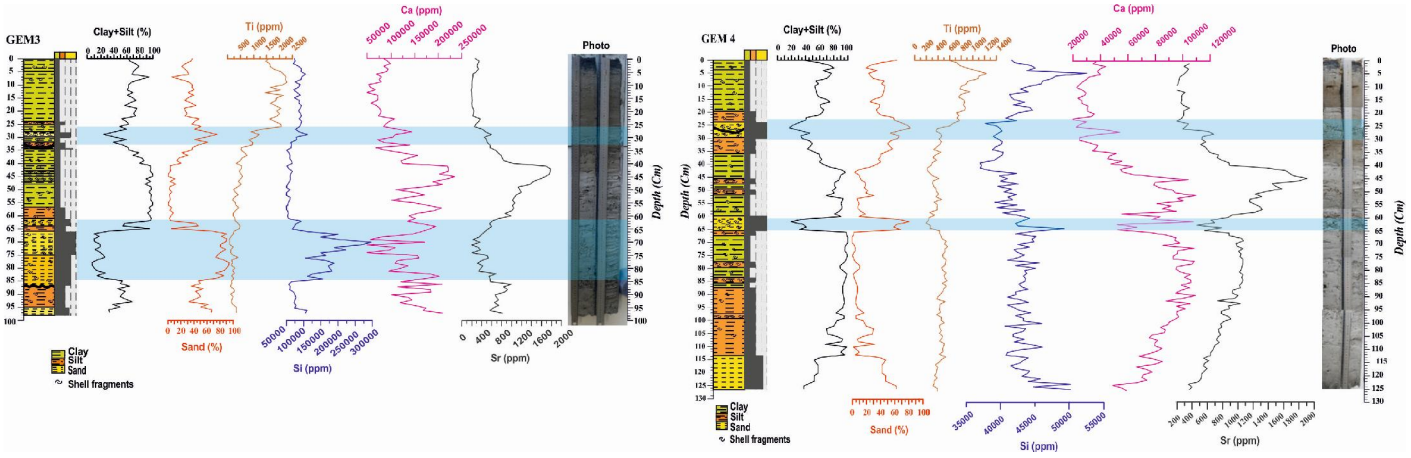

Figure 8: Stratigraphic log and grain size results of GEM3and GEM4 cores compared to the results obtained from the XRF records (Titanium, Silicon, Calcium and Strontium) distributing in the two cores, vs. depth.

https://doi.org/10.5194/nhess-2020-311
Preprint. Discussion started: 3 November 2020

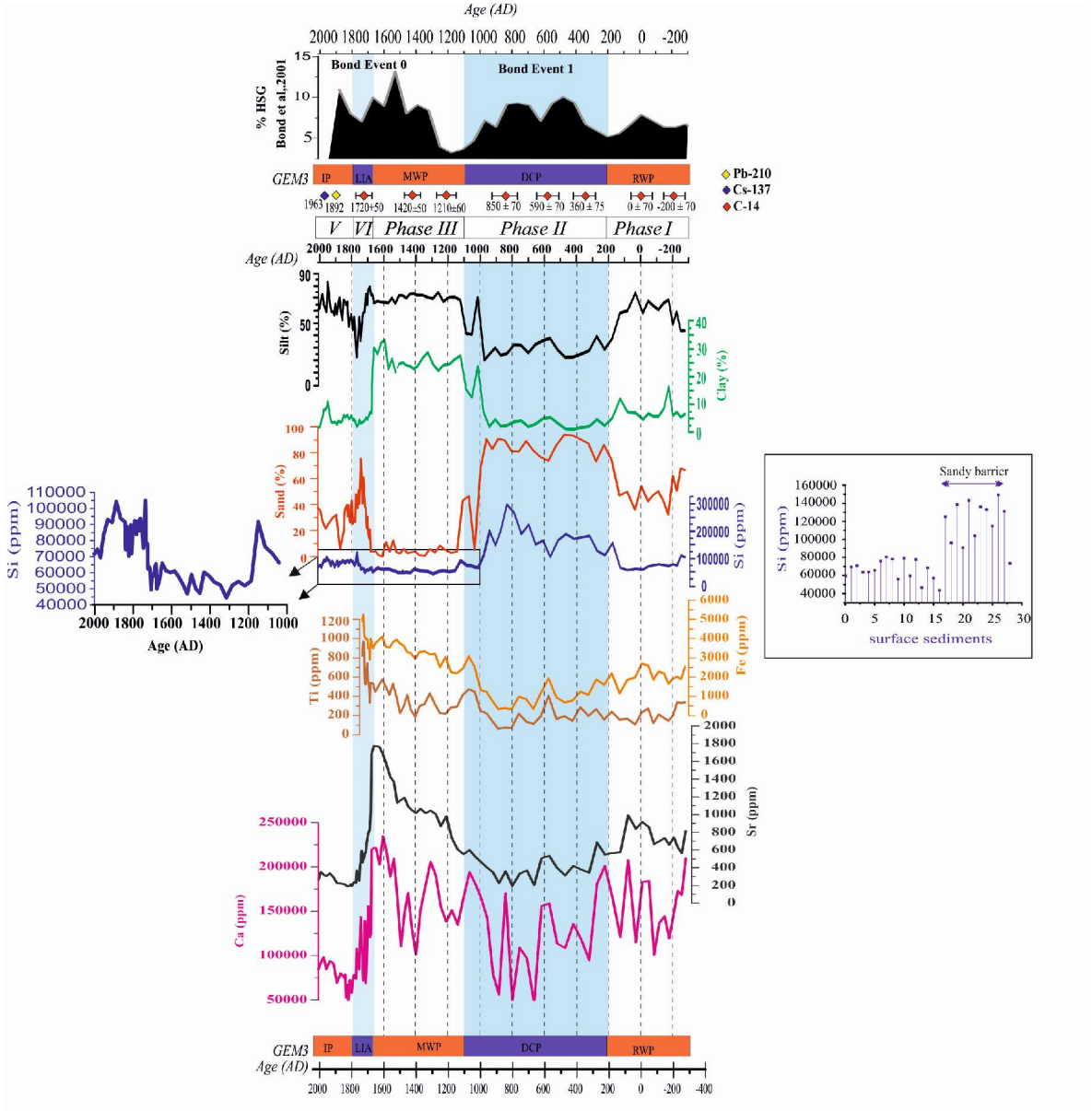

Figure 9: Evolution of grain size population compared to the results obtained from the XRF records (Iron, Calcium, Silicon, Titanium and Strontium) distributing in the GEM3 core, vs. age from -300 till 2012 AD. The two blue bands indicate a period of the Lagoon opening.

465

https://doi.org/10.5194/nhess-2020-311
Preprint. Discussion started: 3 November 2020

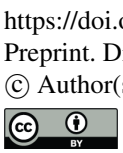

Natural Hazards and Earth System Sciences
Discussions

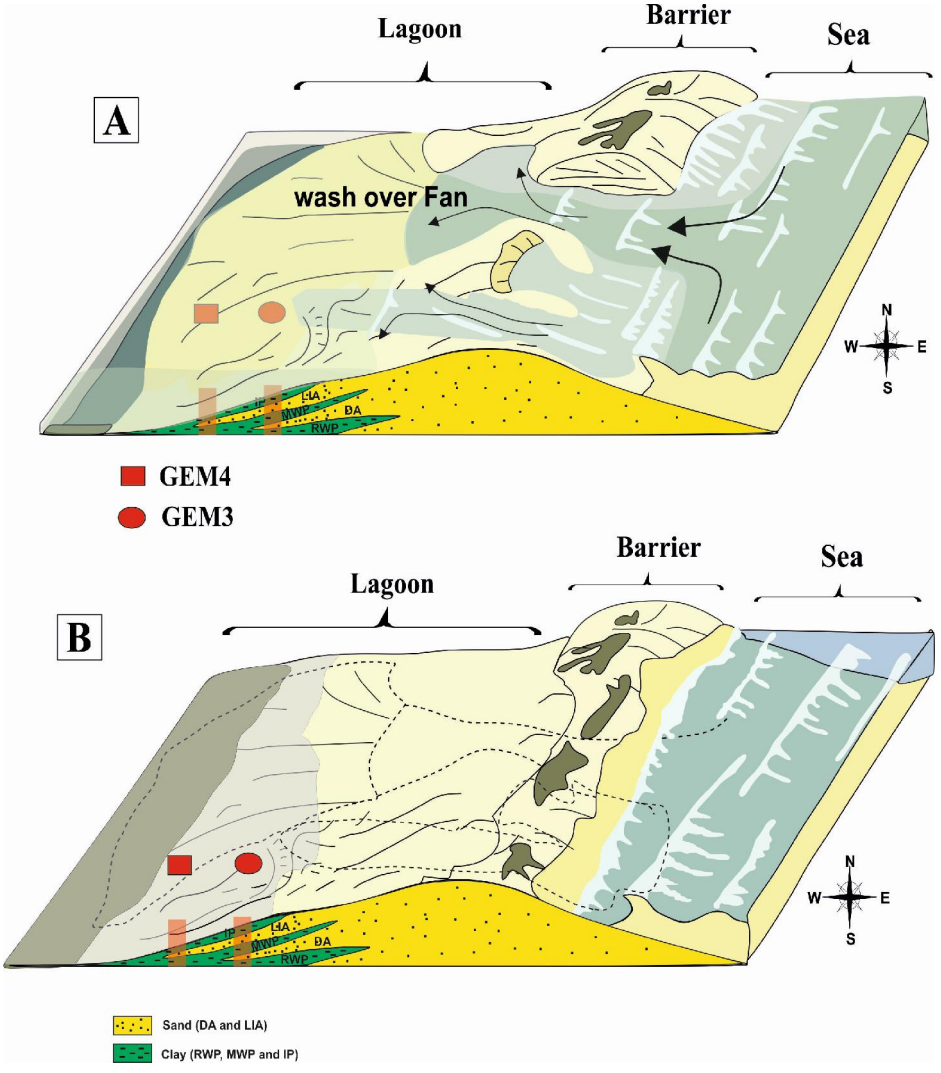

Figure 10: 3D diagram of the lagoon Ghar el Melh evolution since 1690 AD to 2012 AD. (A) Opening of the sandy lido and deposition of the washover in the lagoonal sediment (From 1690 to 1760 Cal AD). (B) Reclosure of the lagoon (From 1760 to 2012 Cal AD).

https://doi.org/10.5194/nhess-2020-311
Preprint. Discussion started: 3 November 2020

Natural Hazards and Earth System Sciences Discussions

Tables

Tab.1. ^{14}C data for shells from GEM3. The model ages were determined by the Oxcal. The ^{14}C ages are calculated and calibrated using the curve of Marine 13 calibration with reservoir age.

Labo code	Mollusk used	Depth (cm)	$\delta^{13}C$ (‰)	^{14}C ages (BP)	Ages (AD) of Clam model
SacA 42679	*Cerastodermaglaucum*	42	-0.8	565±30	1720
SacA 42685	*Cerastodermaglaucum*	54	1.5	930±30	1420
SacA 42683	*Cerastodermaglaucum*	60	0.2	1195±30	1210
SacA 42681	*Cerastodermaglaucum*	70	0.2	1535±30	850
SacA 42680	*Cerastodermaglaucum*	76	1.4	1830±30	590
SacA 42686	*Cerastodermaglaucum*	80	0.6	2015±30	360
SacA 42684	*Cerastodermaglaucum*	88	-1.1	2350±30	0
SacA 42682	*Cerastodermaglaucum*	93	-1.4	2490±30	-200

Tab.2. ^{14}C data for shells from GEM4. The model ages were determined by the Oxcal. The ^{14}C ages are calculated and calibrated using the curve of Marine 13 calibration with reservoir age.

Labo code	Mollusk used	Depth (cm)	$\delta^{13}C$ (‰)	^{14}C ages (BP)	Ages (AD) of Clam model
SacA42676	*Cerastodermaglaucum*	40	-3.7	490±30	1709
SacA42675	*Cerastodermaglaucum*	45	1.8	615±30	1621
SacA42673	*Cerastodermaglaucum*	58	0.3	1181±30	1160
SacA42672	*Cerastodermaglaucum*	72	-2.9	2545±30	-242
SacA42674	*Cerastodermaglaucum*	85	-4.3	2660±30	-408
SacA42678	*Cerastodermaglaucum*	101	-6.6	2625±30	-525
SacA42677	*Cerastodermaglaucum*	110	-4.8	2725±30	-642

Tab.3. ^{14}C age of recent pre-bomb mollusk samples in GEM3 core. The reservoir age R(t) and Δ R were calculated using the $^{210}Pbex$ date

Labo code	^{210}Pb age (AD)	^{14}C year (BP)	Tree-ring ^{14}C age (BP) IntCall 13	Reservoir age R(t) (year)	Model age (Marine 13 curve)	Δ R (year)
SacA44506	1845	450±30	114±8	363	453±23	2